0273-2289/99/82/0227/$13.75

Catalytic and Spectroscopic Properties of Cytochrome-*c*, Horseradish Peroxidase, and Ascorbate Oxidase Embedded in a Sol-Gel Silica Matrix as a Function of Gelation Time

Isabella Savini,[1] Roberto Santucci,[1] Almerinda Di Venere,[1] Nicola Rosato,[1,2] Giorgio Strukul,[3] Francesco Pinna,[3] and Luciana Avigliano*,[1]

[1]Dipartimento di Medicina Sperimentale e Scienze Biochimiche, Università di Roma Tor Vergata, via di Tor Vergata 135, 00133 Rome, Italy, E-mail: avigliano@uniroma2.it; [2]AFaR:IRCCS, Centro S. Giovanni di Dio-FBF, 25100 Brescia, Italy; and [3]Dipartimento di Chimica, Università di Venezia, 30123 Vemezie, Italy

Received August 10, 1999; Revised November 19, 1999; Accepted November 22, 1999

Abstract

In this study, we investigated the optical features of the redox metal-dependent proteins cytochrome-*c*, horseradish peroxidase (HRP), and ascorbate oxidase embedded in a sol-gel-processed silica matrix as a function of gelation time. Circular dichroism, absorbance, and fluorescence spectroscopies revealed that the sol-gel process affects the complex structure of the dimeric ascorbate oxidase (although the prosthetic coppers still remain bound to the enzyme) but not that of monomeric cytochrome-*c* and HRP. Any modifications in ascorbate oxidase occurred in the initial gelation phase; the drying process induced no further alterations and the enzyme remained stable for months. Unfolding-refolding experiments on cytochrome-*c* revealed severely restricted motility in the protein moiety in the *xerogel*, the concentrated matrix that forms after drying. The diffusion time of the solvent within the matrix, which regulated the enzyme-substrate reaction rate, depended on the thickness of the monolith, not on the dryness of the specimen.

*Author to whom all correspondence and reprint requests should be addressed.

Index Entries: Sol-gel; tetramethoxysilane; cytochrome-*c*; ascorbate oxidase; horseradish peroxidase.

Introduction

Over the past decade, more attention has been focused on the embedding of biomolecules in silicate glass formed by the sol-gel method *(1)*. This technique produces a biochemically active material that is optically transparent, porous, and permeable to small reactants and therefore suitable for use as biocatalysts or optically based biosensors. Several proteins and enzymes, such as cytochrome-*c*, superoxide dismutase *(2)*, $NADP^+$-dependent dehydrogenases *(3)*, horseradish peroxidase (HRP) *(4)*, trypsin *(5)*, and glucose oxidase *(6)*, have been successfully embedded and their catalytic properties retained.

Although many studies have been performed on the catalytic activity, little is known about their structural properties. The sol-gel method is particularly useful because the matrix is polymerized in physiological pH solutions and at room temperature. However, several factors, including the alkoxysilane precursor used for the matrix preparation, the alcohol released by precursor hydrolysis, and the solvent evaporation during gel drying, can alter the enzyme structure. The microstructure of the matrix itself changes at various stages during the sol-gel process (referred to in the literature as *gel*, *aged gel*, *xerogel*, or *glass*, but these terms are sometimes used indiscriminately), and this can also affect the properties of the embedded biomolecules. The purpose of our study was to identify the structural properties of various proteins embedded in sol-gel matrices at different stages of development.

We investigated the structural and redox properties of three metallo proteins—cytochrome-*c*, HRP, and ascorbate oxidase—embedded in sol-gel matrix, as a function of gelation time. Cytochrome-*c* is a 12.5-kDa monomer. It contains a heme in the active site that is covalently bound to two cysteines by a thioether bond; the axial ligands of the heme iron in the native state are a histidine and a methionine. HRP is a monomeric hemoprotein (44 kDa) *(7)* widely used in the field of biosensors, because of its high specificity for hydrogen peroxide *(8)*. Ascorbate oxidase is a 140-kDa homodimer. Each subunit is made of three distinct domains and contains four copper ions, as shown by X-ray crystallography *(9)*. The copper ions belong to three different types, classified as type 1, 2, and 3 according to their spectroscopic and catalytic properties *(9)*. Ascorbate oxidase is specific toward ascorbate (vitamin C) oxidation and is thus an effective analytical tool. It has been used to quantify ascorbate in different biological applications, including clinical and food analysis, and to remove ascorbate, which interferes with the estimations of other molecules in analytical systems, such as urinary oxalate *(10)*, serum creatine *(11)*, triglycerides *(12)*, and glucose *(13)*. In some applications, ascorbate oxidase has been physically embedded in calcium-alginate gel beads *(14)* or immobilized on CH-Sepharose 4B via carbodiimide *(15,16)*.

The spectroscopic features of the embedded proteins that we observed using circular dichroism (CD), absorbance, and fluorescence techniques indicate that the sol-gel process induced a limited denaturation of dimeric ascorbate oxidase during the initial gelation phase, but did not induce structural changes in cytochrome-*c* and HRP at any stage. The rigid glasslike matrix, formed when the drying phase was complete, did not affect the structural and redox properties but limited protein moiety motility within the matrix.

Materials and Methods

Chemicals

Ascorbate oxidase from *Cucurbita* species and guanidine hydrochloride (GdHCl) were purchased from Boehringer Mannheim (Mannheim, Germany); cytochrome-*c* from horse heart type VI, type VI-A HRP, pyrogallol, and sodium azide were purchased from Sigma (St. Louis, MO); L-ascorbic acid sodium salt, EDTA, tetramethoxysilane (TMOS), HCl, hydrogen peroxide, and Tris (hydroxymethyl)-aminomethane were purchased from Fluka (Buchs, Switzerland); and 1-anilino-8-naphthalenesulfonic acid (ANS) was purchased by Molecular Probes (Eugene, OR).

Encapsulation of Proteins in Silica Gel

Proteins were embedded using the sol-gel procedure of Ellerby et al. *(2)* with minor modifications. Cytochrome-*c*, HRP, or ascorbate oxidase was dissolved in 0.01 *M* Tris-HCl buffer, pH 8.6, and dialyzed overnight in the same buffer. The sol-gel stock solution was prepared at 4°C by mixing TMOS (5.3 mL), distilled water (1.15 mL), and HCl (0.07 mL of a 0.04 *M* solution), and stirring until the sol phase was formed (about 10 min). At this time, 1.8 mL of protein solution (range of concentration = micrograms to milligrams per milliliter) was added to 1.2 mL of the sol stock solution (final pH 6.2). The mixture was immediately transferred to 3-mL polystyrene cuvets. The gel phase formed within a few minutes. Samples were stored at room temperature for 48 h in cuvets sealed with Parafilm, and then air-dried. After 2 wk, a transparent blue (ascorbate oxidase) or red (cytochrome-*c*, HRP) glasslike monolith, one third the volume of the initial solution ($7 \times 7 \times 21$ mm), formed; we refer to this matrix as *aged gel*. When this monolith was immersed in buffer solution to halt the drying process, no further shrinkage was observed. Samples left to dry for 4 wk reduced to a final volume one eighth that of the initial solution ($4.5 \times 4.5 \times 18$ mm), forming a matrix that we refer to as *xerogel*; no further shrinkage was observed throughout the storage of the sample (usually 6 mo). In some experiments, a volume of 1 mL or less of protein-TMOS mixture was transferred to a 1-mL cuvet and processed. In any case, the aged gel and xerogel were the samples whose volume was reduced to one third and to one eighth of the initial volume, respectively. When immersed in buffers, the xerogel monoliths occasionally fractured, but this did not occur with the aged-gel monoliths.

The properties of the xerogel containing 1 mg of each protein were tested. The nitrogen adsorption-desorption isotherms were measured at 196°C with a Micromeritics ASAP 2010 apparatus (Norcross, GA). Prior to measurement, the sample was degassed at 25°C for 18 h. In any event, a BET surface area of 530 m^2/g was detected. The mesopore size distribution was essentially unimodal with an average pore diameter of about 6–9 nm.

Redox Activity

The monolith containing 0.75 mg of cytochrome-*c* (corresponding to an initial concentration of 20 μ*M*) was immersed in 0.1 *M* phosphate buffer, pH 7.0, containing 1 m*M* EDTA. A reduction in cytochrome-*c* was obtained by adding 100 excess ascorbic acid over the protein; oxidation was obtained by adding 200 excess ferricyanide. The reaction was recorded spectrophometrically (UV/VIS spectrophotometer Lambda 18; Perkin-Elmer, Norwalk, CT) in the wavelength range of 450–650 nm.

HRP activity was measured by recording the increase in absorbance at 450 nm caused by the formation of purpurogallin from pyrogallol, in 0.01 *M* K-phosphate buffer, pH 6.0, and in the presence of 1 m*M* pyrogallol and 5 m*M* H_2O_2. The monolith containing 50 μg of HRP was placed in a total reaction volume of 10 mL, and at fixed times, aliquots of the reaction mixture were analyzed by measuring their absorbance at 450 nm; the reaction mixture was stirred constantly throughout the experiment.

Ascorbate oxidase activity was measured spectrophotometrically at 25°C by recording the decrease in absorbance at 265 nm caused by ascorbate oxidation (E = 14 $mM^{-1}\,cm^{-1}$), in 0.1 *M* K-phosphate buffer, pH 6.0, containing 1 m*M* EDTA. When high ascorbic acid concentrations were used, the absorbance was recorded at 288 nm. The activity of 50 μg of ascorbate oxidase embedded in the monolith was measured using a procedure similar to the one for HRP. The K_m value was obtained by fitting the initial reaction velocity vs substrate concentration data directly to the Michaelis-Menten equation. The K_m value was obtained by nonlinear regression analysis using a Sigma Plot 1.01 program (Jandel, Chicago, IL).

CD Measurements

CD measurements were made in the Soret region (380–450 nm) using a Jasco J-710 spectropolarimeter (Tokyo, Japan) equipped with a PC data processor.

Steady-State Fluorescence Measurements

Steady-state fluorescence was measured with a single-photon counting spectrofluorometer (ISS, model K2, Champaign, IL). The bandwidth of excitation and emission monochromators was set to 4 nm to maximize the fluorescence signal and to keep the scattering as low as possible. The emission spectrum of 0.25 mg of ascorbate oxidase (corresponding to an initial concentration of 0.62 μ*M*) in 0.1 *M* K-phosphate buffer (pH 6.0), or in

silicate matrix was obtained at an excitation of 280 nm. Under the same conditions, the fluorescence intensity of the gel without the protein was negligible.

The emission spectra of ascorbate oxidase treated with ANS were obtained at an excitation of 350 nm, at which the absorbance of ANS was 0.04. To monitor the ANS binding to ascorbate oxidase in the first 24 h of the gelation process, the sample was prepared by mixing 10 excess ANS to the ascorbate oxidase solution immediately before gel embedding. Alternatively, the monolith was immersed in a buffer solution containing 10 times as much ANS with respect to ascorbate oxidase and left to equilibrate overnight.

All measurements were made at 22°C by thermostating the sample holder with an external circulating water bath.

Results and Discussion

The structural and redox properties of cytochrome-*c*, HRP, and ascorbate oxidase were monitored as a function of gel aging, i.e., during the first 24–48 h, after 2 wk (aged gel), and after 4 wk (xerogel). Typical experiments were repeated every 4 wk for a maximum of 6 mo. No differences were observed among samples aged for 4 wk or 6 mo, stored either "dry" or immersed in buffer at room temperature. Similarly, no differences in the spectroscopic features of embedded proteins were observed in dry monoliths or in those immersed in buffer solution.

Cytochrome-c

The CD spectrum of embedded cytochrome-*c* recorded in the Soret region (this 400- to 450-nm region probes both the heme microenvironment and the protein backbone to which the heme is covalently bound) was similar to that of cytochrome-*c* in phosphate buffer solution, indicating that the structure of cytochrome-*c* did not change on encapsulation. In particular, a negative Cotton effect was observed at 416 nm, and a positive one at 408 nm, similar to that seen in the native protein (Fig. 1, spectrum a). The absorption spectra showed that the embedded cytochrome-*c* underwent reversible oxidation-reduction reactions on treatment with ferricyanide or ascorbate. However, the features of the absorption spectra were typical of cytochrome-*c* in its oxidized or reduced state, indicating that all the protein molecules were accessible to reagents in both aged and xerogel monoliths (data not shown). The reactions were completed in about 1 h in aged gel and in about 0.5 h in xerogel, indicating that the rate of diffusion of the solvent depended mostly on the path length (7 mm in aged-gel monolith vs 4.5 mm in xerogel monolith) and not on the microstructure of the matrix.

To determine how the glassy matrix affects the behavior of the protein, we investigated the denaturation process of embedded cytochrome-*c*. To achieve this, we added 3.5 *M* GdHCl solution to the cuvet containing the aged-gel block; this denaturant concentration is known to induce full, rapid denaturation of the protein in solution. We observed important changes in

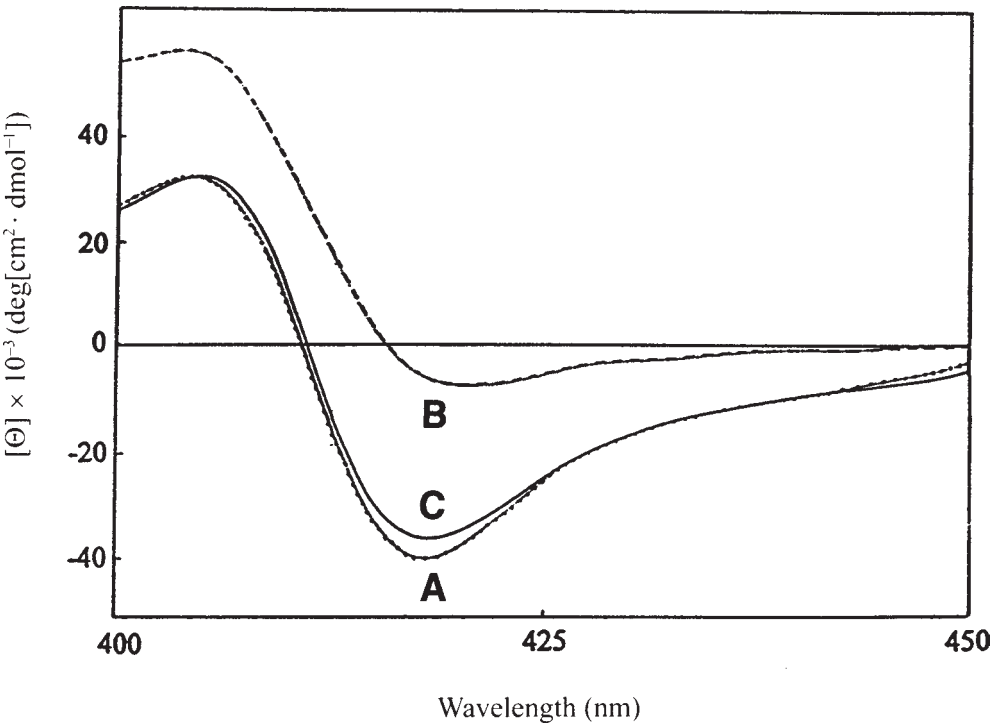

Fig. 1. Soret CD spectra of 25 µg of cytochrome-*c* embedded in gel aged for 2 wk (a) in the absence and (b) in the presence of 3.5 *M* GdHCl and (c) after removal of the denaturant. The buffer was 0.1 *M* K-phosphate, pH 7.0.

the Soret CD spectrum of the entrapped protein on denaturation. In particular, the 416-nm Cotton effect disappeared whereas the 408-nm Cotton effect increased (Fig. 1, spectrum b). At variance with cytochrome-*c* in solution, whose CD spectrum on mixing was typical of that of the denatured protein, the embedded protein underwent a slow denaturation process (50–60 min). The reverse process, i.e., refolding of the denatured protein, was obtained when the denaturant solution was replaced with fresh phosphate buffer. It took 30 min for cytochrome-*c* to recover its native structure (Fig. 1, spectrum c). Only partial denaturation (about 20%) occurred in xerogel after incubation for 24 h with 3.5 *M* GdHCl, indicating that this matrix prevented the protein backbone from unfolding. This study shows that reversible conformational transitions are permitted in aged gel but are restricted in xerogel. A similar restriction in wet gel has been documented for serum albumin *(17,18)* and hemoglobin, whose conformational changes on reaction with molecular oxygen were prevented when the protein was embedded *(19,20)*.

Horseradish Peroxidase

HRP embedded in silica matrix retained its ability to catalyze substrate oxidation by H_2O_2. However, the reaction rate, as measured by the

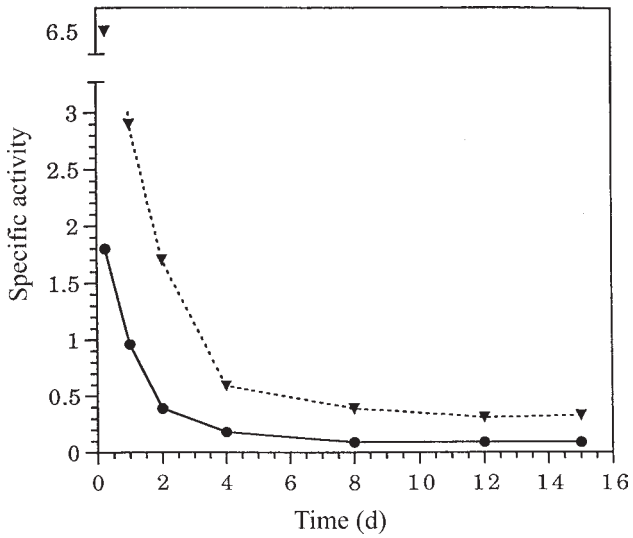

Fig. 2. Specific activity of (▼) 50 µg of gel-embedded HRP or (●) 50 µg of gel-embedded ascorbate oxidase as a function of gel aging. Activity is expressed as a percentage of that of the enzyme in solution, as calculated from the initial velocity of substrate oxidation. Conditions were as in Materials and Methods.

slope of the curve for pyrogallol oxidation, was low in comparison with that measured with HRP in solution (Fig. 2). This decrease occurred in the first 48 h of the sol-gel process; thereafter the activity remained constant.

The Soret CD (not shown) and absorbance spectra of embedded HRP and native protein were identical, indicating that immobilization in the gel material did not alter the structural integrity of the protein.

HRP is an enzyme that catalyzes the H_2O_2-dependent one-electron oxidation of a large number of substrates. Heme is the protein active site; in the ground state, the heme-iron oxidation state is Fe(III). The two-equivalent oxidized Compound I forms on reaction with H_2O_2; in the presence of a reductant substrate, Compound I rapidly reconverts to HRP via another intermediate, Compound II. In the absence of a reductant substrate and in the presence of some excess of H_2O_2 (up to 25:1 H_2O_2:protein), HRP has weak catalase activity *(21,22)*. In this case, H_2O_2 acts as both an oxidant and a reductant: the protein is first oxidized to Compound I, which, being a strong oxidant, induces H_2O_2 to act as a reductant, yielding HRP and oxygen via Compound II. We investigated the catalase activity of HRP embedded in aged gel and in xerogel by monitoring the formation and stability of the reaction intermediates.

Figure 3 shows the changes induced by an excess of H_2O_2 (25:1 molar ratio) in the Soret absorbance spectrum of HRP in solution (Fig. 3A) or embedded in aged gel (Fig. 3B). On the addition of H_2O_2 to HRP in solution, the absorbance band centered at 403 nm decreased to about one half, and a shoulder centered at 416–418 nm appeared. This was consistent with the formation of Compound I (whose spectrum, centered at 403 nm, was about

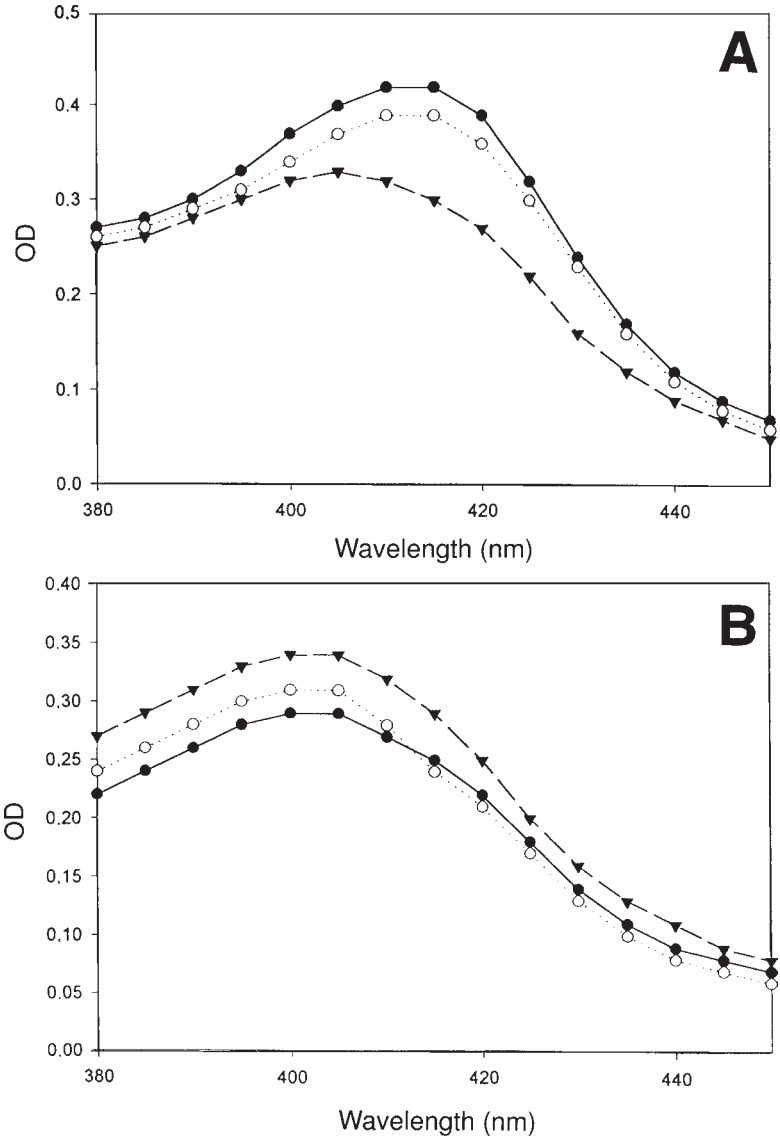

Fig. 3. Soret absorbance spectra of HRP in solution **(A)** or in gel aged for 2 wk **(B)** after the addition of H_2O_2 (25:1 H_2O_2:protein molar ratio). (▼), Mixing time; (○), after 15 min; (●), after 60 or 120 min. The buffer was 0.1 *M* K-phosphate, pH 7.0.

half as intense as that of HRP in the ground state) and Compound II (whose spectrum, centered at 416 nm, was as intense as that of HRP in the ground state). In the absence of a reductant substrate, Compound II gradually stabilized during the first hour, as indicated by the marked increase in the absorbance band centered at 416 nm. Then the reaction appeared to proceed slower owing to the absence of relevant changes in the absorbance spectrum, at least for the following 2 h. However, the spectrum typical of the native protein was mostly recovered after 24 h (Fig. 4A).

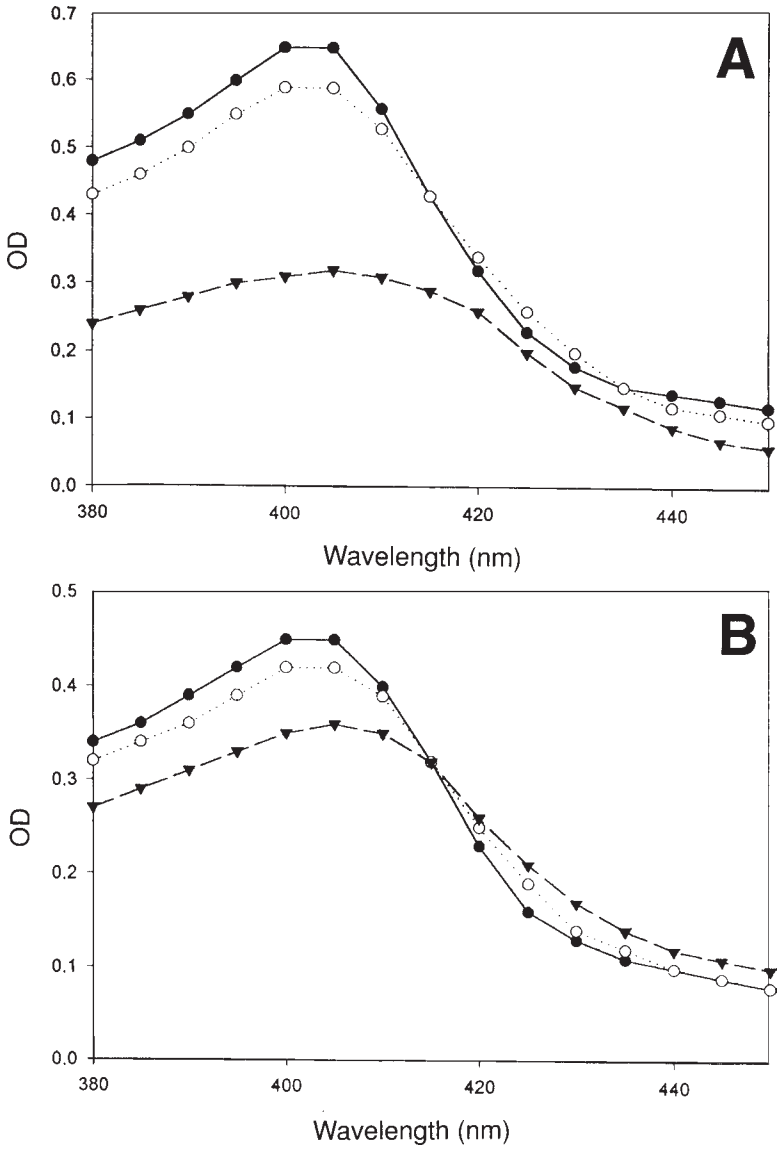

Fig. 4. Soret absorbance spectra of HRP in solution **(A)** or in gel aged for 2 wk **(B)** in the absence (●) and in the presence of H_2O_2 (10:1 H_2O_2:protein molar ratio). (▼), Mixing time; (○), after 24 h. The buffer was 0.1 *M* K-phosphate, pH 7.0.

By contrast, the reaction of gel-embedded HRP with H_2O_2 proceeded much slower (Fig. 3B). In fact, the addition of H_2O_2 to the buffer induced less dramatic changes in the Soret absorbance spectrum of the embedded protein. After mixing, the intensity of the Soret absorbance band centered at 403 nm decreased only slightly (approx 20%), and no shoulder was observed at 416 nm. This was consistent with a partial formation of Compound I and the absence of Compound II. During the first hour after mixing, the band centered at 403 nm gradually decreased, and a weak shoulder

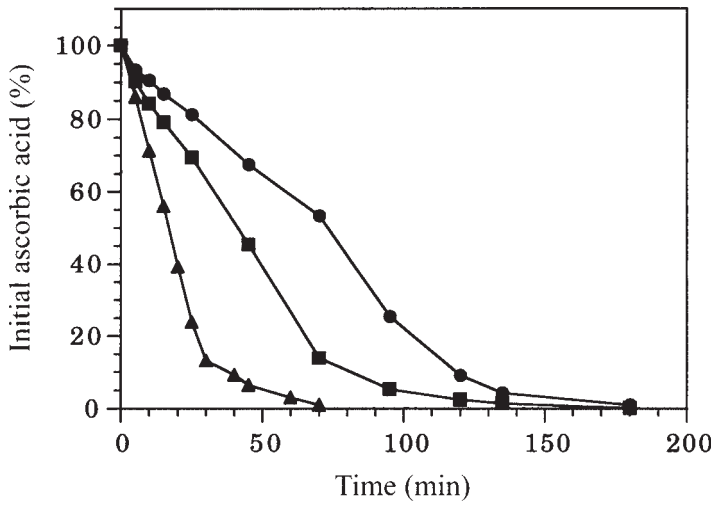

Fig. 5. Enzymatic oxidation of ascorbic acid by 50 µg of ascorbate oxidase encapsulated in a xerogel aged for 4 wk. Ascorbic acid concentration: (▲), 50 µ*M*; (■), 0.2 m*M*; (●), 1 m*M*. Other conditions were as in Materials and Methods.

centered at 416 nm appeared. The results obtained on embedded HRP indicate that, although the gel matrix did not alter the structural integrity of the embedded HRP, it greatly influenced the reaction rate, which was about 50% faster in xerogel than in aged gel, but in both cases much slower than in solution, indicating that the matrix limited the solvent diffusion. This was also confirmed by the color gradient observed in the protein-containing monolith after the addition of H_2O_2 to the buffer; whereas the inside of the glass block remained brown (HRP was still in the ground state), the interfacial surface turned green (indicating formation of Compound I). Interestingly, the spectrum recorded after 24 h was typical of the native protein (Fig. 4B), thus indicating that the HRP ground state was fully recovered, as observed for the protein in solution.

Ascorbate Oxidase

Ascorbate oxidase embedded in silica matrix retained its ability to catalyze ascorbic acid oxidation by molecular oxygen (Fig. 5). The K_m for ascorbate was unaffected (0.14 m*M* for ascorbate oxidase in glass vs 0.12 m*M* in solution). Instead, the reaction rate, as measured by the slope of the curve for ascorbate oxidation, was low in comparison with that measured with ascorbate oxidase in solution (Fig. 2). This trend was similar to that monitored with HRP; however, the effect was enhanced with ascorbate oxidase.

Figure 6 shows the visible absorbance spectra of ascorbate oxidase in solution and in a gel aged for 24 or 48 h. The blue band, ascribed to type 1 Cu, was unmodified, and the 330-nm shoulder, related to the trinuclear site formed by type 2 Cu and by the diamagnetic type 3 Cu pair, disappeared after embedding. This picture was not modified by further aging and drying. On reduction with ascorbate, the blue band was fully bleached, indi-

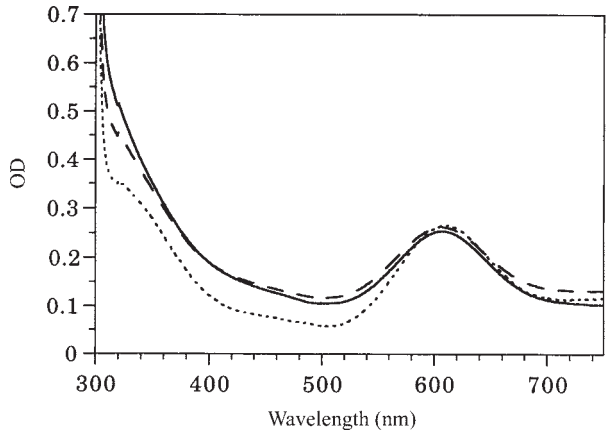

Fig. 6. Absorption spectrum of 3.8 mg/mL of ascorbate oxidase in solution (- - - -), in gel aged for 24 h (— — —), or in gel aged for 48 h (——).

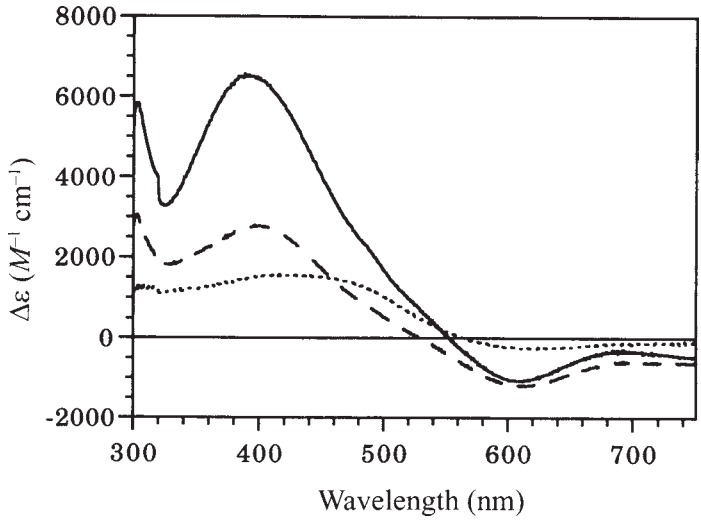

Fig. 7. Titration with azide of ascorbate oxidase embedded in gel aged for 4 wk. The experiment was performed in 0.01 *M* phosphate buffer, pH 6.0, by adding concentrated solutions of azide to a monolith containing 6 mg of ascorbate oxidase and allowing the solution to equilibrate at room temperature. (- - - -), 25 excess azide over the protein, 4 h of incubation; (— — —), 100 excess azide over the protein, 4 h of incubation; (——), 2600 excess azide over the protein, overnight incubation.

cating that the type 1 Cu was still accessible to the substrate when ascorbate oxidase was embedded in aged gel or xerogel. It is well known that the 330-nm band is significantly affected by solvent perturbation or by copper removal from the trinuclear site *(23)*. To test the latter possibility, we investigated the reactivity of embedded ascorbate oxidase with azide, a strong inhibitor of ascorbate oxidase that binds stepwise to coppers of the trinuclear site *(24–26)*; therefore, the ascorbate oxidase–azide complex may be indicative of the status of the trinuclear center. Figure 7 shows represen-

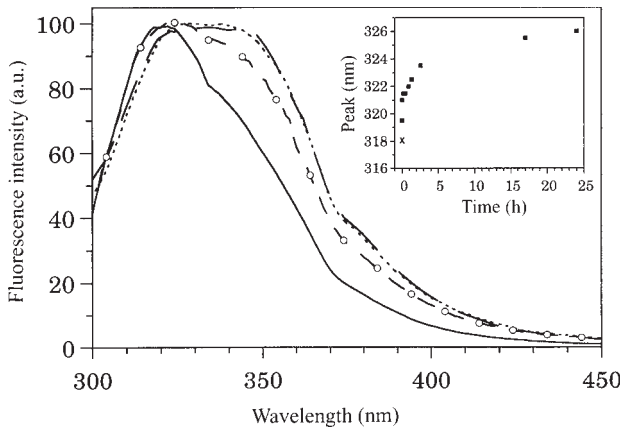

Fig. 8. Steady-state fluorescence spectra of ascorbate oxidase, excited at 280 nm, in buffer (——), in gel aged for 24 h (○), 2 wk (- - - -), and 4 wk (— — —). All spectra are normalized to 100. Conditions were as in Materials and Methods. **(Inset)** Ascorbate oxidase fluorescence peak position in the initial gelation phase (■) as a function of time compared to the peak position of native ascorbate oxidase in buffer (×).

tative differential spectra obtained by azide titration of ascorbate oxidase embedded in xerogel. A broad increase between 400 and 500 nm was observed when low quantities of azide were added, and an intense band developed at about 400 nm when large amounts of the anion were added. These optical features were quite similar to those generated by azide binding to native protein in solution *(24,25)*. Together these observations indicate that the sol-gel and drying process induced structural changes in ascorbate oxidase, although the copper atoms, even those more labile and exposed to the solvent such as type 2 and type 3 coppers, remained bound to the protein.

Information on the tertiary structure of the ascorbate oxidase may be obtained through its fluorescence features, including both the intrinsic fluorescence of protein tryptophans and the extrinsic fluorescence of protein-bound ANS (a fluorophore that increases its quantum yield on binding to hydrophobic regions of a protein) *(27)*.

The steady-state emission spectra of ascorbate oxidase in buffer solution, in 24-h aged gel, in 2-wk aged-gel, and in xerogel, normalized to 100 at their maximum, as seen in Fig. 8. Under the same conditions, the fluorescence intensity of the gel without the protein was negligible and is thus not reported. The intrinsic fluorescence of the ascorbate oxidase in gel was wider and red-shifted in comparison to the same protein in buffer, and its maximum was at about 330 nm. These spectral characteristics are similar to those of the stable, dimeric, scarcely reactive intermediate form found at 1 *M* GdHCl during the chemical unfolding of the ascorbate oxidase *(27)*.

Previous studies demonstrated that ascorbate oxidase does not bind to ANS in its native form or in its 4 *M* GdHCl-treated, unfolded monomeric form; however, it does bind to ANS in its 1 *M* GdHCl-induced state *(27)*.

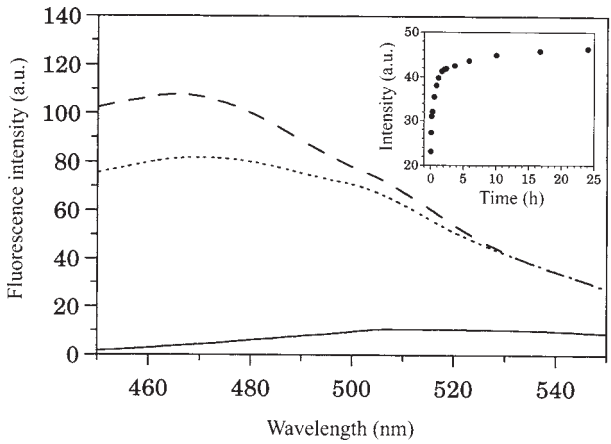

Fig. 9. Fluorescence emission spectra of ANS in buffer (——) and in gels aged for 24 h (- - - -) or 2 wk (— — —). Conditions were as in Materials and Methods. **(Inset)** ANS fluorescence intensity at 475 nm as a function of time during the first 24 h.

The emission spectra of ANS-treated ascorbate oxidase in gels aged for 24 h or 2 wk, and the emission spectrum of the ANS gel without the protein were normalized to 100 (*see* Fig. 9). The emission of the ANS in the gel without the protein was very low and red-shifted in comparison to the emission of ANS bound to the ascorbate oxidase in gel. This behavior clearly indicates that ANS freely diffuses in the gel matrix and binds preferentially to the exposed hydrophobic cavities of the protein molecules. The ANS-binding experiments are in agreement with those reported in Mei et al. *(27)* with GdHCl and suggest a structural analogy between the 1 *M* GdHCl-induced state and the gel-induced state of ascorbate oxidase. There is, in fact, a large increase (about 10 times) in the fluorescence intensity of ANS bound to the ascorbate oxidase in gel in comparison to the emission of the ANS in the gel without the protein. In a similar experiment on native ascorbate oxidase in solution, the increase in ANS fluorescence was negligible with respect to free ANS in buffer (data not shown).

The aforementioned effects may be explained by a partial loosening of the tertiary structure of the gel-embedded ascorbate oxidase that exposes more hydrophobic patches on its surface in comparison to the native protein in buffer. This conformational modification, as shown by changes in intrinsic and extrinsic fluorescence of ascorbate oxidase, parallels the gelation process during the first 24 h (inset of Figs. 5 and 6). Further polymerization and drying did not induce additional modifications in the protein.

Conclusion

Previous investigations have reported on the properties of the embedded protein as a function of the evolving sol-gel matrix. However, in some cases, the aging process was described only in terms of time and not in

terms of dryness of the specimen *(17,18)*. In other cases, only catalytic *(1,5)* or structural *(2,17–20)* protein properties were tested. Consequently, reports in the literature make it difficult to correlate enzymatic activity, protein structure, and matrix stage. The present study provides deeper insight on this point, which is extremely important for the biotechnological application of the sol-gel matrix.

Our data indicate that ascorbate oxidase, a large protein with quaternary structure and complex tertiary structure, lost some of its native folding, even in freshly formed gel. This does not occur with the smaller, monomeric protein cytochrome-*c* and HRP. It is well known that small proteins withstand chemical or thermal denaturation to a greater degree than the large multidomain proteins, in which bonds at the interface between the structural domains can loosen without unfolding the protein backbone. The modification of the protein structure and the decrease in the reaction rate occurred in the first 24–48 h of the sol-gel process, indicating that the polymerization phase is critical for protein encapsulation. Our data also indicate that the matrix does not affect the dynamics of the entrapped protein at the stage of aged gel. Sterically, restrictions occur only at the stage of xero-gel, as indicated by the cytochrome-*c* unfolding-refolding experiments; however, the embedded protein was still fully accessible to small reactants.

In conclusion, structural as well as kinetic analysis should be used to investigate eventual modifications caused by the sol-gel process, and therefore lead to the optimization of the systems used. Each protein examined showed the same features when embedded in the aged-gel or xerogel matrices. It may be advantageous, however, to block the process at the aged-gel stage, given that further drying increases the probability that the monolith will fracture when subjected to immersion cycles, and that the embedded protein is still mobile in the aged-gel matrix, a particularly significant fact considering that an enzyme may undergo allosteric structural changes during its activity.

Finally, this study also showed that the ascorbate oxidase–silica composite material can be used as a possible detection device for the measurement of ascorbate, as well as for its removal from biological fluids. Native ascorbate oxidase oxidized L-ascorbate quite efficiently (k_{cat} = 7500/s in buffer solution, pH 6.0–8.0); therefore, despite a limited loss of activity and the slow diffusion of the substrate into the matrix, micrograms of embedded ascorbate oxidase oxidized physiological concentrations of ascorbate within minutes. Furthermore, although reduced, the specific activity remained stable over time and the K_m, and thus the affinity of ascorbate oxidase for ascorbate, remained unaltered.

Acknowledgments

This research was supported by grants from the Italian MURST and from the Italian CNR target projects, MADESS II.

References

1. Avnir, D., Braun, S., Lev, O., and Ottolenghi, M. (1994), *Chem. Mater.* **6,** 1605–1614.
2. Ellerby, L. M., Nishida, C. R., Nishida, F., Yamanaka, S. A., Dunn, B., Valentine, J. S., and Zink, J. I. (1992), *Science* **255,** 1113–1115.
3. Yamanaka, S. A., Dunn, B., Valentine, J. S., and Zink, J. I. (1995), *J. Am. Chem. Soc.* **117,** 9095, 9096.
4. Wu, S., Lin, J., and Chan, S. I. (1994), *Appl. Biochem. Biotechnol.* **47,** 11–20.
5. Shtelzer, S., Rappoport, S., Avnir, D., Ottolenghi M., and Braun, S. (1992), *Biotechnol. Appl. Biochem.* **15,** 227–235.
6. Hartenett, A. M., Ingersoll, C. M., Baker, G. A., and Bright, F. (1999), *Anal. Chem.* **71,** 1215–1224.
7. Dunford, H. B. (1991), in *Peroxidases in Chemistry and Biology*, vol. 2, Everse, I., Everse, K. E., and Grisham, M. B., eds., CRC Press, Boca Raton, FL, pp. 1–24.
8. Ruzgas, T., Csoregi, E., Emneus, J., Gorton, L., and Marko-Varga, G. (1996), *Anal. Chim. Acta* **330,** 123–128.
9. Messerschimdt, A., Ladenstein, R., Huber, R., Bolognesi, M., Avigliano, L., Petruzzelli, R., Rossi, A., and Finazzi-Agrò, A. (1992), *J. Mol. Biol.* **224,** 179–205.
10. Crawford, G. A., Mahoney, J. F., and Györy, A. Z. (1985), *Clin. Chim. Acta* **147,** 51–57.
11. Suzuki, M. and Yoshida, M. (1984), *Clin. Chim. Acta* **140,** 289–294.
12. Freemantle, J., Freemantle, M. J., and Badrik, T. (1994), *Clin. Chem.* **40,** 950, 951.
13. Anzai, J., Takeshita, H., Kobayashi, Y., Osa, T., and Hoshi, T. (1998), *Anal. Chem.* **70,** 811–817.
14. Esaka, M., Suzuki, K., and Kubota, K. (1985), *Agric. Biol. Chem.* **49,** 2955–2960.
15. Stevanato, R., Avigliano, L., Finazzi-Agrò, A., and Rigo, A. (1985), *Anal. Biochem.* **149,** 537–542.
16. Greenway, G. M. and Ongomo, P. (1990), *Analyst* **115,** 1297–1299.
17. Edmiston, P. L., Wambolt, C. L., Smith, M. K., and Saavedra, S. S. (1994), *J. Colloid Interface Sci.* **163,** 395–406.
18. Jordan, J. D., Dunbar, R. A., and Bright, V. F. (1995), *Anal. Chem.* **67,** 2436–2443.
19. Shibayama, N. and Saigo, S. (1995), *J. Mol. Biol.* **251,** 203–209.
20. Shibayama, N. and Saigo, S. (1999), *J. Am. Chem. Soc.* **121,** 444, 445.
21. Arnao, M. B., Acosta, M., del Rio, J. A., Varòn, R., and Garcia-Canovas, F. (1990), *Biochim. Biophys. Acta* **1041,** 43–47.
22. Baynton, K. J., Bewtra, J. K., Biswas, N., and Taylor, K. E. (1994), *Biochim. Biophys. Acta* **1206,** 272–278.
23. Morpurgo, L., Graziani, M. T., Marcozzi, G., and Avigliano, L. (1993), *J. Inorg. Biochem.* **51,** 641–647.
24. Casella, L., Gullotti, M., Pallanza, G., Pintar, A., and Marchesini, A. (1988), *Biochem. J.* **251,** 411–466.
25. Cole, J., Avigliano, L., Morpurgo, L., and Solomon, E. I. (1991), *J. Am. Chem. Soc.* **113,** 9080–9089.
26. Messerschmidt, A., Luecke, H., and Huber, R. (1993), *J. Mol. Biol.* **230,** 997–1014.
27. Mei, G., Di Venere, A., Buganza, M., Vecchini, P., Rosato, N., and Finazzi-Agrò, A. (1997), *Biochemistry* **36,** 10,917–10,922.